International Journal of Pharmaceutics 629 (2022) 122379

Contents lists available at ScienceDirect

International Journal of Pharmaceutics

journal homepage: www.elsevier.com/locate/ijpharm

A liposomal formulation of simvastatin and doxorubicin for improved cardioprotective and anti-cancer effect

Ronja Bjørnstad [a,b,1], Ingeborg Nerbø Reiten [a,1], Kaja Skålnes Knudsen [a], Jan Schjøtt [c,d], Lars Herfindal [a,*]

[a] Centre for Pharmacy, Department of Clinical Science, University of Bergen, Norway
[b] Hospital Pharmacy in Western Norway, Bergen, Norway
[c] Department of Clinical Science, University of Bergen, Bergen, Norway
[d] Department of Medical Biochemistry and Pharmacology, Haukeland University Hospital, Bergen, Norway

ARTICLE INFO

Keywords:
Cardiotoxicity
Doxorubicin
Drug repurposing
Liposomes
Cancer
Simvastatin

ABSTRACT

Anthracyclines such as doxorubicin (Dox) are the preferred chemotherapeutics for several cancers. However, Dox-induced cardiotoxicity limits its therapeutic potential. Liposomal encapsulation of Dox has been used for patients with risk to develop Dox induced cardiotoxicity but does not surpass the efficacy of the unencapsulated drug. Statins are widely used as cholesterol lowering drugs and have also demonstrated cardioprotective activity in cancer patients undergoing Dox therapy. We developed a liposome loaded with Dox and simvastatin (Sim) and investigated their effect on cardiomyocytes and zebrafish larvae. Furthermore, we investigated if the doses required for cardioprotection compromised the cytotoxicity of Dox in mammary and prostate cancer cells. Combination of Sim and Dox reduced ROS generation in cardiomyocytes, both given as free drugs, or co-encapsulated in liposomes. In contrast, Sim potentiated ROS-generation and cytotoxic activity of Dox towards cancer cells also when co-encapsulated in liposomes. In zebrafish larvae, Sim treatment reduced Dox-induced cardiac affection, and the liposomes did not induce any sign of Dox-induced cardiotoxicity. Our results show that liposomal co-encapsulation of Sim and Dox can be an efficient way of further reducing the risk of cardiotoxic events of liposomal Dox, while retaining, or even potentiating the anti-cancer effect of Dox.

1. Introduction

Doxorubicin (Dox) is one of the most versatile anti-cancer drugs in use today. The main anti-cancer action of the drug is believed to be blocked DNA replication by topoisomerase II inhibition, but also generation of cellular stress by elevated levels of reactive oxygen species (ROS) (Gewirtz, 1999). Despite its widespread use as an anti-cancer drug, Dox is associated with several adverse effects, including cardiotoxicity, which can ultimately result in reduced left ventricular ejection fraction (LVEF), congestive heart failure, and death (Alexander et al., 1979). The frequency of Dox-induced cardiotoxicity in patients is found to be dose-related, which limits the cumulative doses that patients can receive, restricting the therapeutic potential of the drug (Swain et al., 2003; Lefrak et al., 1973). The underlying molecular mechanisms of the cardiotoxic effects are not fully understood but Dox-induced ROS accumulation and apoptosis in cardiomyocytes is suggested to be important (Goffart et al., 2004; Davies and Doroshow, 1986; Wolf and Baynes, 2006; Octavia et al., 2012; Angsutararux et al., 2015; Cappetta et al., 2017). Cardiomyocytes are found to be particularly sensitive to elevated ROS levels, and it is believed that their anti-oxidative defence systems are already saturated by endogenous oxidative metabolism (Cappetta et al., 2017).

Abbreviations: ACN, acetonitrile; DCFDA, 2′,7-dichlorofluoresceindiacetate; DLS, dynamic light scattering; Dox, Doxorubicin; dpf, days post fertilization; EW, embryo water; HEPC, hydrogenated egg phosphatidylcholine; hpf, hours post fertilization; hpi, hours post injection; i.v., intravenous; LVEF, left ventricular ejection fraction; MQ, milli-Q water; MS-222, Ethyl 3-aminobenzoate methanesulfonate; PCE, Pericardial oedema; PdI, polydispersity index; PEG, polyethylene glycol; PEG-PE, 1,2-distearoyl-sn-glycero-3-phosphoethanolamine-N-[methoxy (polyethylene glycol)-2000] (ammonium salt); PLD, polyethylene glycol coated liposomal doxorubicin; ROS, Reactive oxygen species; Sim, Simvastatin; TEM, transmission electron microscope; TFA, trifluoroacetic acid.

* Corresponding author at: Department of Clinical Science, Jonas Lies vei 87, N-5021 Bergen, Norway.
E-mail address: lars.herfindal@uib.no (L. Herfindal).

[1] These authors contributed equally.

https://doi.org/10.1016/j.ijpharm.2022.122379
Received 19 July 2022; Received in revised form 19 October 2022; Accepted 4 November 2022
Available online 9 November 2022

Several attempts have been made to develop treatment protocols that can limit anthracycline- and especially Dox-induced cardiotoxicity (Bansal et al., 2019). Polyethylene glycol (PEG) coated liposomal Dox (PLD) has been in use since 1995 under the brand name Doxil® or Caelyx® (Barenholz, 2012). Liposomal encapsulation of drugs can improve pharmacokinetics, circulation time and biodistribution by protecting the drug from rapid elimination. Perhaps most important, however, is that liposomes can reduce the harmful effects of drugs on normal tissues and organs, and more precisely deliver the drugs to tumour tissues (Wang and Wang, 2014). A phase III study of patients with metastatic breast cancer comparing treatment with PLD and free Dox found that there was a substantially lower risk of developing cardiomyopathy following treatment with the liposomal formulation while the anti-cancer efficacy was comparable (O'Brien et al., 2004). However, PLD has unfortunately not increased the overall survival of patients and has not been able to replace the use of free Dox (Barenholz, 2012).

Currently, dexrazoxane is the only U.S. Food and Drug Administration (FDA)-approved cardioprotective agent against anthracycline-induced cardiomyopathy (reviewed in Bansal et al., 2019). Dexrazoxane binds to iron and prevents anthracycline-iron complexes and therefore iron-dependent oxidative stress in the myocardium. This permits patients to receive higher cumulative doses of Dox without developing intolerable cardiac side effects (Speyer et al., 1992). However, the use of dexrazoxane is restricted, due to studies showing that it may cause secondary malignancies (Tebbi et al., 2007) and reduce the anti-cancer effect of Dox in breast cancer (Swain et al., 1997) although the evidence is conflicting (Bansal et al., 2019; Ganatra et al., 2019). Another class of drugs that is shown to prevent Dox-induced cardiotoxicity are the 3-hydroxy-3-methylglutaryl-coenzyme A reductase inhibitors, commonly known as statins. Statins are cholesterol-lowering drugs used for the prevention of cardiovascular diseases, but their possible role as cardioprotectants in anthracycline therapy is believed to be due to their pleiotropic effects and/or antioxidant properties and not related to their cholesterol-lowering effects (Liao and Laufs, 2005; Henninger and Fritz, 2017). In the clinic, statin use was observed to lower the mean reduction in LVEF following anthracycline therapy (Feleszko et al., 2000; Riad et al., 2009; Acar et al., 2011), and two independent clinical trials have investigated if treatment with statins in combination with adjuvant anthracycline treatment preserves normal heart function in breast cancer patients, in a 15-week (clinicaltrials.gov, NCT02096588) or 24-month (clinicaltrials.gov, NCT01988571) time frame. In addition to their possible cardioprotective role, statins have been proven to inhibit cellular proliferation through induction of apoptosis in cancer cells (Crick et al., 1998; Jakóbisiak et al., 1991; Park et al., 2001; Maltese and Sheridan, 1985; Rao et al., 1999; Mueck et al., 2003; Seeger et al., 2003). In the case of breast cancer, in vivo studies in mouse mammary tumour models demonstrated decreased tumour formation and inhibition of metastasis (Alonso et al., 1998; Farina et al., 2002) and several studies suggested that long-term statin use reduces the risk of cancers (Blais et al., 2000; Islam et al., 2017; Wu et al., 2015; Tan et al., 2017; Singh et al., 2013; Graaf et al., 2004; Shai et al., 2014).

In this study, we wanted to explore the cardioprotective effects of the statin simvastatin (Sim) in Dox therapy by co-encapsulating the two drugs in PEGylated liposomes. Sim is a prodrug, and when administered orally, the extensive liver metabolism causes <5 % of the drug to reach systemic circulation (Schachter, 2005). In the treatment of hypercholesterolemia, the target organ is the liver, and systemic drug delivery is not desired. In relation to Dox therapy, it is crucial that Sim reaches systemic circulation since the target organ is the heart. The cardioprotective and anti-cancer effects of our liposomes were studied in H9c2 cardiomyoblast, and the MCF7 mammary and PC3 prostate adenocarcinoma cancer cell lines. Zebrafish larvae were also used to investigate Sim as a cardioprotective agent in Dox-induced cardiotoxicity. The zebrafish has become a frequent model to observe toxic effects of drugs or toxins (Bambino and Chu, 2017), and previous studies have shown the heart function of zebrafish are affected by drugs known to cause cardiotoxic effects in humans (Zhu et al., 2014; Dyballa et al., 2019; Maciag et al., 2022).

2. Materials and methods

2.1. Materials

Water was from a Milli-Q water purification system (Millipore Corporation, Bedford, MA, USA). 1,2-distearoyl-*sn*-glycero-3-phosphoethanolamine-N-[methoxy (polyethylene glycol)-2000] (ammonium salt) (PEG-PE) and Lipoid E PC-3 Hydrogenated egg phosphatidylcholine (HEPC) were from Lipoid GmbH (Ludwigshafen, Germany). Doxorubicin (Dox) hydrochloride was obtained from Accord Healthcare (Gothenburg, Sweden). 2′,7-dichlorofluoresceindiacetate (DCFDA) was from ThermoFischer Scientific, Waltham, MA, USA. MycoAlert™ was obtained from BioNordika AS (Oslo, Norway). HPLC grade acetonitrile (ACN) was from VWR International (Radnor, PA, USA). Formaldehyde, phosphate buffered saline tablets (PBS), ammonium sulphate, simvastatin, cell proliferation reagent WST-1, HPLC grade methanol, ethyl 3-aminobenzoate methane-sulfonate (MS-222), DMEM medium (D6546), penicillin/streptomycin, foetal bovine serum, Bisbenzimide H33342 trihydrochloride (Hoechst) and uranyl acetate were from Sigma-Aldrich (St. Louis, MO, US).

2.2. Preparation of liposomes co-loaded with Sim and Dox

Liposomes were made by thin-film hydration followed by extrusion. A lipid film was produced using 54.6 mg HEPC and 4.5 mg PEG-PE dissolved in chloroform and evaporating the solvent using a rotary evaporator. For liposomes loaded with Sim, 1.75 or 7.5 mg Sim (3 or 12.7% w/w Sim/lipids) dissolved in chloroform was added to the lipid mix before evaporation. The resulting film was rehydrated in 1 mL 225 mM ammonium sulphate (pH 5.3) preheated to 70 °C. The flask was alternating heated and vortexed for at least 15 min until there was no trace of the film left on the glass. After hydration, the samples containing Sim were centrifuged at 10000*g* at 20 °C for 15 min and the supernatant collected. Liposome extrusion was performed using a Mini Extruder from Avanti Polar Lipids, Inc. (Alabaster, AL, US) with Whatman® Nucleopore Track-Etched membrane filters. Extrusion was performed 11 times each through 0.8, 0.4, 0.2, and 0.1 μm Whatman filters at 70 °C. Next, the suspension buffer was changed to PBS (pH 8) by size exclusion chromatography through a 1 cm (i.d.) and 20 cm long column filled with Sephadex G50 Medium from GE Health Science (Pittsburg, USA) and equilibrated with PBS (pH 8). After gel-filtration, liposomes were loaded with Dox using the acid-precipitation method (Fritze et al., 2006). Dox was added to up to 20 % w/w of the lipid concentration and incubated for one hour at 70 °C while gently shaken, followed by 4 °C overnight. Liposomes used for in vitro experiments were gel filtered once more to remove any non-encapsulated drug, while liposomes to be used for injection in zebrafish larvae were unfiltered to maintain high concentration of liposomal Dox in the suspension.

2.3. Liposome characterization

The size and polydispersity index (PdI) of the liposomes were analysed by dynamic light scattering (DLS) using a Zetasizer Nano ZS (Malvern Instruments Ltd., Malvern, UK), with the Zetasizer Software (version 7.10). The liposomes were diluted in PBS (pH 7.4) before DLS measurements. Imaging of liposomes was performed with a JEOL 1011 transmission electron microscope (TEM) with a MORADA camera using OIS computer system. A small drop of liposome suspension was deposited on a grid and left to settle for one min. The grid was then rinsed by gently placing it onto drops of MQ five subsequent times, for approximately five seconds each, before finally depositing the grid on a drop of 2 % uranyl acetate for ten seconds. Any excess uranyl acetate was removed with paper. The grid was left to dry for at least 24 h before

imaging. ImageJ (Schneider et al., 2012) was used to measure the size of the liposomes from the obtained TEM images. The concentration of lipids in the liposome suspensions was determined using Direct Detect® infrared spectrometer (Merck Millipore, Darmstadt, Germany). Drug content in the liposomes were determined by high performance liquid chromatography (HPLC). The HPLC system used was a HITACHI Chromaster 5160 pump, 5260 autosampler and 5430 diode array detector (Tokyo, Japan) and a Merck L-7614 degasser (Darmstadt, Germany). For Dox quantification, 50 μL of the liposome sample was dried in a vacuum centrifuge and resuspended in ACN/MQ (30/70). From this, 10 μL was injected into a Kromasil C18, 10 μm particle size, 4.6x150 mm column fitted with a 4.6x10 mm guard column of the same stationary phase. For Sim quantification, 5 μL liposome sample was dissolved in 145 μL methanol/MQ (80/20). From this, 5 μL sample was injected onto an Agilent Phenyl-hexyl column, 2.7 μm particle size, 4.6x150 mm. The mobile phase gradients are shown in Table 1, and for both analyses mobile phases were 0.05 % TFA in MQ (A) and 0.05 % TFA in ACN (B) and methanol (C). The chromatograms were recorded at 238 and 236 nm for Sim and Dox, respectively.

2.4. In vitro experiments

2.4.1. Cell culture conditions

The cardiomyoblast cell line H9c2 (ATCC CRL-1446), and the human mammary and prostate adenocarcinoma cell lines MCF7 (ATCC HTB-22) and PC3 (ATCC CRL-1435), respectively, were cultured in DMEM medium, enriched with 10 % foetal bovine serum and 2 mM L-glutamine, and supplemented with 100 IU/mL penicillin and 100 mg/L streptomycin. The cells were cultured in a humidified atmosphere at 37 °C, with 5 % CO_2. During maintenance, the cell lines were cultured until reaching 80 % confluence, upon which they were detached by mild trypsinization, centrifuged, and reseeded in fresh medium at 40 % confluence. After 12 passages, the cells were discarded. Cells were tested for mycoplasma infection using MycoAlert™ every second month. No positive tests were obtained in any cell line during the time of the experiments.

2.4.2. Measurements of ROS-Generation

Assessment of ROS production was performed using the fluorogenic probe 2′,7-dichlorofluoresceindiacetate (DCFDA). Cells were seeded in black 96-well plates with clear bottoms, at 5×10^4 cells/mL at 0.1 mL per well. After 24 h, the cells were washed three times with PBS and added DCFDA (25 μM in serum free medium) and incubated at 37 °C for 30 min. Next, the DCFDA was removed, and cells were added various treatments. Hydrogen peroxide (1 and 20 μM) was used for positive control. The fluorescence intensity was measured every two hours until the ROS values peaked, using a BioTek Synergy H1 Hybrid Multi-Mode Reader (Ex/Em = 485/535 nm, Agilent Technologies, CA, USA).

2.4.3. Assessment of cell cytotoxicity

All cytotoxicity experiments were performed in 96-well plates with 0.1 mL medium/well. For 24 h drug exposure, cells were seeded at 5×10^4 cells/mL and left over-night to attach before adding drugs or control vehicles. The metabolic activity of the cells was measured using the WST-1 Cell Proliferation Assay (Roche Applied Science, Penzberg, Germany). After reading the absorption of the converted tetrazolium product with a Wallac EnVision™ 2103 Multilabel reader at 450 nm (reference 620 nm), the cells were fixed by adding 0.1 mL 4 % buffered (PBS, pH 7.4) formaldehyde containing the DNA-dye Hoechst 33342 (0.01 mg/mL). The presence of apoptotic cells was assessed by evaluating Hoechst-stained nuclei using a UV-microscope (Nikon Diaphot 300 microscope, Melville, NY, USA) (Saraste and Pulkki, 2000) and the fraction of normal nuclei for each treatment were confirmed by the WST-1 results. To find drug interaction, we used two methods. The first was to use isobolographic plots of EC_{50} values of the drugs alone or in combination (Gessner, 1988). If the data from the combination follow a straight line between the EC_{50} values of each drug alone, there is an additive effect of the combination, whereas if the points lie below this line, there is a synergistic or potentiating effect. The second method was to calculate the coefficient of drug interaction (CDI) using Eq. 1, where R is the ratio between the effect of treatment and control. A value around one indicates additive effect, values below 0.7 demonstrate clear synergy, and above one indicates antagonistic effect (Bjørnstad et al., 2019).

$$\mathrm{CDI} = \frac{R_{\mathrm{Combination}}}{R_{\mathrm{Drug1}} \times R_{\mathrm{Drug2}}} \quad (1)$$

Table 1
HPLC Gradients for Dox and Sim Quantification. Gradients of mobile phases A (0.05 % trifluoroacetic acid (TFA) in Milli-Q water), B (0.05 % TFA in acetonitrile) and C (methanol) for doxorubicin (Dox) quantification on a C18 column and simvastatin (Sim) quantification on a phenyl-hexyl column.

Dox quantification							
Time (minutes)	**0**	**1**	**3**	**4**	**5**	**6**	**8**
A (%)	70	70	30	0	0	70	70
B (%)	30	30	70	100	100	30	30
Sim quantification							
Time (minutes)	**0**	**1**	**12**	**13**	**14**	**15**	**20**
A (%)	20	20	0	0	0	20	20
B (%)	0	0	40	100	100	0	0
C (%)	80	80	60	0	0	80	80

2.5. In vivo experiments on zebrafish larvae

2.5.1. Animal care

Zebrafish (Danio rerio) were kept at 28 °C in a 14-hour light, 10-hour dark cycle at The Zebrafish Facility at the Department of Bioscience, University of Bergen. The facility is run according to the European Convention for the Protection of Vertebrate Animals used for Experimental and Other Scientific Purposes. The embryos obtained were of the optically transparent strain Casper (D'Agati et al., 2017). Zebrafish embryo and larvae were kept at 28.5 °C in embryo water (EW) according to general practice (Westerfield, 1995). The zebrafish larvae were kept up to 120 hpf before they were euthanized by cooling on ice for 20 min, followed by freezing at −20 °C.

2.5.2. Intravenous injection of drugs in zebrafish larvae

Thin-walled borosilicate glass capillaries (i.d. 0.78 mm, o.d. 1.0 mm) were pulled using a P-1000 Micropipette puller by Sutter Instruments (Novato, CA, US). The micropipettes were retrogradely filled with the injection solution before being fitted on a Narishige MMN-5 and MMO-220A micromanipulator system (Tokyo, Japan) and connected to an Eppendorf Femtojet 4x microinjector (Hamburg, Germany). The micropipette tip was emerged in a thin layer of groundnut oil and cut using a scalpel. The pressure and injection time were adjusted to obtain a droplet of 4 nL from each injection. The zebrafish larvae were anesthetized in 0.8 mM MS-222 for a minimum of 10 min prior to intravenous (i.v.) injection (Westerfield, 1995). Anaesthetized zebrafish larvae were placed on 2 % w/v agarose gel and injected via the posterior cardinal vein. Unencapsulated Sim could not be injected because of the low aqueous solubility and was dissolved in the EW. The drug was dissolved to 48 mM in DMSO, and further dissolved in EW to desired concentrations.

2.5.3. Determination of toxic effects in zebrafish larvae

To observe the zebrafish larvae and to obtain videos to monitor heart rate (HR) and morphological abnormalities, a Leica M205 stereo microscope combined with Leica DFC3000 G camera and the Leica Application Suite X software (Leica Microsystems GmbH, Wetzlar, Germany) was used. For determination of HR, the number of cardiac contractions were counted for 10 s. To evaluate the condition of the skeletal muscle in the tail of the zebrafish larvae exposed to Sim, the

larvae were categorized into three scores: 1) No effect on skeletal muscle. 2) Mild skeletal muscle affection. 3) Severe skeletal muscle affection. See Fig. 3C for examples of each category. Evaluation of adverse muscle effects were conducted blindly, and in case of doubt, the mildest category was selected.

2.6. Statistical analysis

EC_{50} values were determined by using a four-parameter non-linear regression analyses in SigmaPlot for Windows ver. 14.0 (Systat Software Inc., Palo Alto, CA, USA). Differences between treatments were analysed for significance by One-way analysis of variance (ANOVA). Post-hoc tests were chosen based on Levene's homogeneity of variance test. LSD test was used if there was equal variance between samples and Dunnett's T3 if the variance was unequal. For muscle damage scores we used Kruskal-Wallis non-parametric test for multiple samples. Pairwise comparisons adjusted with Bonferroni correction was used to find differences between groups. The software IBM SPSS statistics for Apple, ver. 25 (IBM Corp., Armonk, NY, USA) was used for all statistical analyses. Significance was defined as $p \leq 0.05$, and all tests were two-tailed.

3. Results

3.1. Dox and Sim can be co-loaded into pegylated liposomes

Sim was dissolved in chloroform together with the lipids. With this method, we obtained a drug loading of Sim of around 9 % when 12.7 mg Sim was added per mg lipid, measured after the liposomes had been gel-filtered to remove non-encapsulated Sim (Table 2). Dox was loaded by the acid precipitation method up to 20 % of the measured lipid concentration. More than 90 % of the added Dox was found in the liposome fraction when subjected to a size exclusion chromatography column (Fig. S1). We also produced a formulation where 3.0 mg Sim/mg lipid was added, which resulted in a drug loading around 5 % (Table 2). These liposomes had non-toxic Sim concentrations in zebrafish larvae and could be loaded with Dox at concentrations that would give cardiotoxic effects if administered as free drug. The liposome diameter was found to be between 140 and 180 nm by DLS, and all had a polydispersity index at 0.10 or lower (Table 2 and Fig. 1 E and F).

The incorporation of Dox in the Sim liposomes did not compromise liposome morphology. TEM images of liposomes loaded with Sim or both Sim and Dox showed unilamellar vesicles (Fig. 1A and B). The diameter of the liposomes measured from the TEM images was lower than measured by DLS (Fig. 1C – F).

Table 2
Liposome characterization. Sim was added per mg lipid before rehydration, while Dox was added per mL liposome suspension. Drug and lipid content was measured by HPLC and Direct Detect spectrometry, respectively. Diameter by intensity and polydispersity index (PdI) was analysed using dynamic light scattering.

Liposomes	Drugs added		Drug loading		Diameter	PdI
	(%, w/w)	(mg/mL)	(mg/mg lipid, %)		(nm)	
	Sim	Dox	Sim	Dox		
Empty	–	–	–	–	147	0.10
Sim	12.7	–	9.3 ± 2.0	–	168	0.09
Sim	3.0	–	5.1 ± 1.7	–	171	0.10
Dox	–	0.5	–	5.8 ± 3.4	144	0.10
Sim-Dox	12.7	0.5	5.7 ± 2.2	15.0 ± 5.6	174	0.06
Sim-Dox	3.0	0.5	5.1 ± 1.7	16.1 ± 2.1	–	–

3.2. The cardioprotective effect of Sim is retained when encapsulated into liposomes

As increased ROS levels are suggested to be important in the cardiotoxic effects of Dox (Lefrak et al., 1973; Goffart et al., 2004; Davies and Doroshow, 1986; Wolf and Baynes, 2006; Octavia et al., 2012; Angsutararux et al., 2015) ROS levels were determined in H9c2 cardiomyoblasts exposed to Dox and Sim, both unencapsulated and liposomal. There was a dose-dependent increase in ROS levels in cardiomyocytes treated with 1 or 20 μM Dox, while 10 μM Sim treatment alone did not affect basal ROS levels in H9c2 cardiomyoblasts (Fig. 2A). Pre-treatment with Sim, followed by treatment with 20 μM Dox, however, significantly reduced the Dox-induced ROS generation in the H9c2 cells. Cells treated with 1 μM Dox and 10 μM Sim only had a modest, non-significant increase in ROS levels compared to untreated cells (Fig. 2A).

When formulated into PLD, Dox significantly increased ROS-production in the H9c2 cardiomyoblast using both 1 and 20 μM (Fig. 2B). However, the ROS generation from 20 μM PLD was significantly less pronounced relative to unencapsulated Dox. The ROS generation was additionally decreased when the cells were pre-treated with 10 μM unencapsulated Sim (Fig. 2B). Next, we measured ROS-generation in cardiomyocytes treated with liposomes co-loaded with Dox and Sim. At 20 μM Dox and 10 μM Sim, ROS generation was significantly lowered compared to 20 μM PLD alone. Sim-Dox liposomes at 1 μM Dox and 0.5 μM Sim had similar ROS levels to Dox-loaded liposomes alone (Fig. 2B).

Several studies have showed that statins can enhance drug-induced apoptosis in cancer cells (Crick et al., 1998; Jakóbisiak et al., 1991; Park et al., 2001; Maltese and Sheridan, 1985; Rao et al., 1999; Mueck et al., 2003; Seeger et al., 2003). It was therefore of interest to find if Sim also enhanced the Dox-induced cytotoxicity towards cardiomyoblasts. We found a dose-dependent reduction in cell viability of Dox treated H9c2 cells with an EC_{50} value of 8.1 ± 1.2 μM (Fig. 2C), whereas Sim showed less cytotoxic activity with EC_{50} of 39.5 ± 2.1 μM (Fig. 2D). Incubation with non-toxic concentrations of Sim (1 or 10 μM, Fig. 2C) did not affect the Dox-induced cytotoxicity in cardiomyoblast relative to treatment with Dox alone, demonstrated by the drug interaction analysis (Fig. 2E).

PLD had lower cytotoxicity towards cardiomyocytes compared to free drug (Fig. 2F and 2C, respectively). Liposomes loaded with Sim showed no cytotoxicity at the concentrations tested, and the liposomes co-loaded with Sim and Dox did not show increased cytotoxicity compared to the PLD (Fig. 2F). Since it was not possible to obtain EC_{50} values for the Sim-loaded liposomes, the hyperbolic method for drug interaction could not be performed, and the CDI (Eq. 1, Methods section 2.4.3) was calculated. From this, no interaction, neither synergistic nor antagonistic was found between encapsulated Sim and Dox on H9c2 cells.

We next tested to which extent our drugs and formulations affected the heart of zebrafish larvae. Preliminary testing revealed that a single 4 nL i.v. injection of 2 ng Dox reduced the HR of zebrafish larvae after 24 h when injected at three dpf at the protruding mouth developmental stage (Kimmel et al., 1995) (data not shown). When dissolved in EW, we found that Sim was lethal at concentrations above 200 nM (Fig. 3A) and increased incidence of pericardial oedema and muscle damage was observed at concentrations of 40 nM and above (Fig. 3B-D). We also found that Sim caused an increase in HR from 10 nM after 24 h Sim exposure, but the heart rate was normalized after 48 h (Fig. 3E). Based on these results we decided to use 10 or 20 nM Sim for 18 h pre-treatment prior to a Dox injection and to register the HR 24 h thereafter.

When monitoring the heart rate of zebrafish larvae treated with the drugs alone or in combination, we found that recipients of Dox alone or Dox in combination with 10 nM Sim pre-treatment had reduced HR compared to the control group (Fig. 4A). Pre-treatment with 20 nM Sim prior to a Dox injection, however, hindered the HR reduction of Dox, and

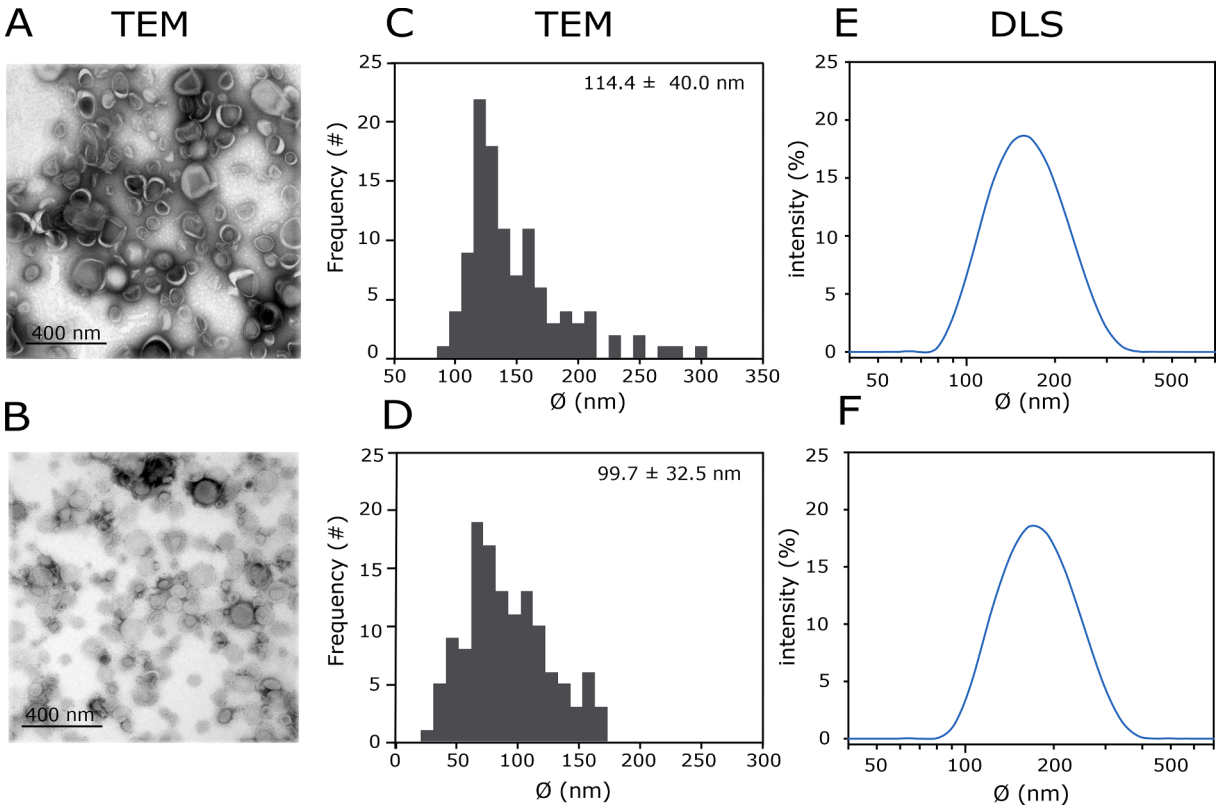

Fig. 1. Morphology and Size of PEGylated Liposomes Analysed by TEM and DLS. A and B: Transmission electron microscopy (TEM) images of uranyl-acetate-stained liposomes loaded with simvastatin (Sim, A) and liposomes co-loaded with Sim and doxorubicin (Dox, B). C and D: Distribution of the diameter for liposomes loaded with Sim (C), or with Sim and Dox (D) measured from the TEM images. E and F: Size distribution of the same liposomes as in C and D, measured by dynamic light scattering (DLS).

the group was equal to those treated with 20 nM Sim alone. Sim alone at 10 or 20 nM did not alter zebrafish HR compared to the control group.

A preliminary dose-escalation test revealed that zebrafish larvae receiving a 4 nL injection of 0.37 mM liposomal Sim and above developed muscle damage and PCE 48 hpi (data not shown). Accordingly, we used 0.19 mM liposomal Sim to investigate the cardioprotective effect in relation to Dox toxicity. We found that injection of empty liposomes caused a modest, but significant reduction in heart rate compared to larvae injected with PBS, but no other signs of cardiotoxicity, such as pericardial oedema. At 48 hpi, none of the liposomal formulations affected the HR compared to empty liposomes, whereas unencapsulated Dox reduced HR (Fig. 4B). The frequency of Dox induced congestive heart failure in the clinic correlates with cumulative amount of drug received over time (Swain et al., 2003). We therefore injected the larvae both at two- and three dpf and observed HR 24 h after the second injection. However, HR was still not affected by any of the liposomal formulations (Fig. 4C).

3.3. *Co-encapsulation of Sim in Dox-liposomes potentiates the cytotoxic effect in cancer cell lines*

In line with our observations for the H9c2 cardiomyocytes (Fig. 2), both 1 and 20 μM Dox significantly increased ROS levels in the MCF7 cells (Fig. 5A). However, Sim did not attenuate Dox induced ROS production in MCF7 cancer cells. Instead, co-treatment with 10 μM Sim and 1 or 20 μM Dox increased ROS production. Additionally, a significant increased ROS generation was observed for the MCF7 cells exposed to Sim alone relative to the control, something that was not observed in the H9c2 cells (Fig. 5A and 2A, respectively).

The liposomal formulations of Dox and Sim had a similar, but less pronounced cytotoxic effect towards the MCF7 cells, compared to that of the free drugs (Fig. 5B). The liposomal formulations with 20 μM Dox showed a reduced effect on the MCF7 cell ROS production when compared to treatment with free Dox, to a lower degree compared to that observed in the H9c2 cardiomyoblasts. Also, inclusion of Sim in the Dox-loaded liposomes did not cause a reduction in ROS generation in the MCF7 cells as was observed for the cardiomyoblasts (Fig. 5B).

When studying the cytotoxicity, we found that in the MCF7 cells, Dox alone had an EC_{50} of 5.0 ± 0.4 μM, but co-treatment with 1 and 10 μM Sim lowered the EC_{50} values to 4.0 ± 0.5 and 2.0 ± 0.3 μM, respectively (Fig. 5C). Importantly, treatment with Sim alone in the cancer cells did not cause any cytotoxic activity at concentrations up to 10 μM (Fig. 5D), and the drug combination analysis demonstrated that non-toxic concentrations of Sim had a potentiating effect on Dox cytotoxicity (Fig. 3E).

In line with this, liposomes loaded with both Sim and Dox gave a lower EC_{50} value compared to liposomes loaded with Dox only in MCF7 cells (Fig. 5F). This was evident with concentrations of Sim which were non-toxic to the cells alone (Fig. 5F, black trace). Calculations of CDI showed a synergistic effect between Sim and Dox also when co-encapsulated in liposomes (Fig. 5F).

We wanted to verify whether the observed cytotoxic effects on MCF7 cells could be replicated in other cancer cell lines and tested the same drugs and formulations on the PC3 prostate adenocarcinoma cell line. Similar to our findings on the MCF7 cells (Fig. 5), we found that both 1 and 10 μM Sim lowered the EC_{50} value when added as a pre-treatment prior to Dox exposure compared to Dox alone (Fig. 6A). These Sim concentrations were not cytotoxic on their own (Fig. 6B). The drug interaction analysis confirmed a potentiating effect of Sim (Fig. 6C).

Furthermore, the liposomal formulations also gave similar results as observed for MCF7, with the Sim-Dox-liposomes increasing PC3 cytotoxicity (EC_{50} for Dox, 4.0 ± 1.5 μM) compared to PLD alone (EC_{50} for

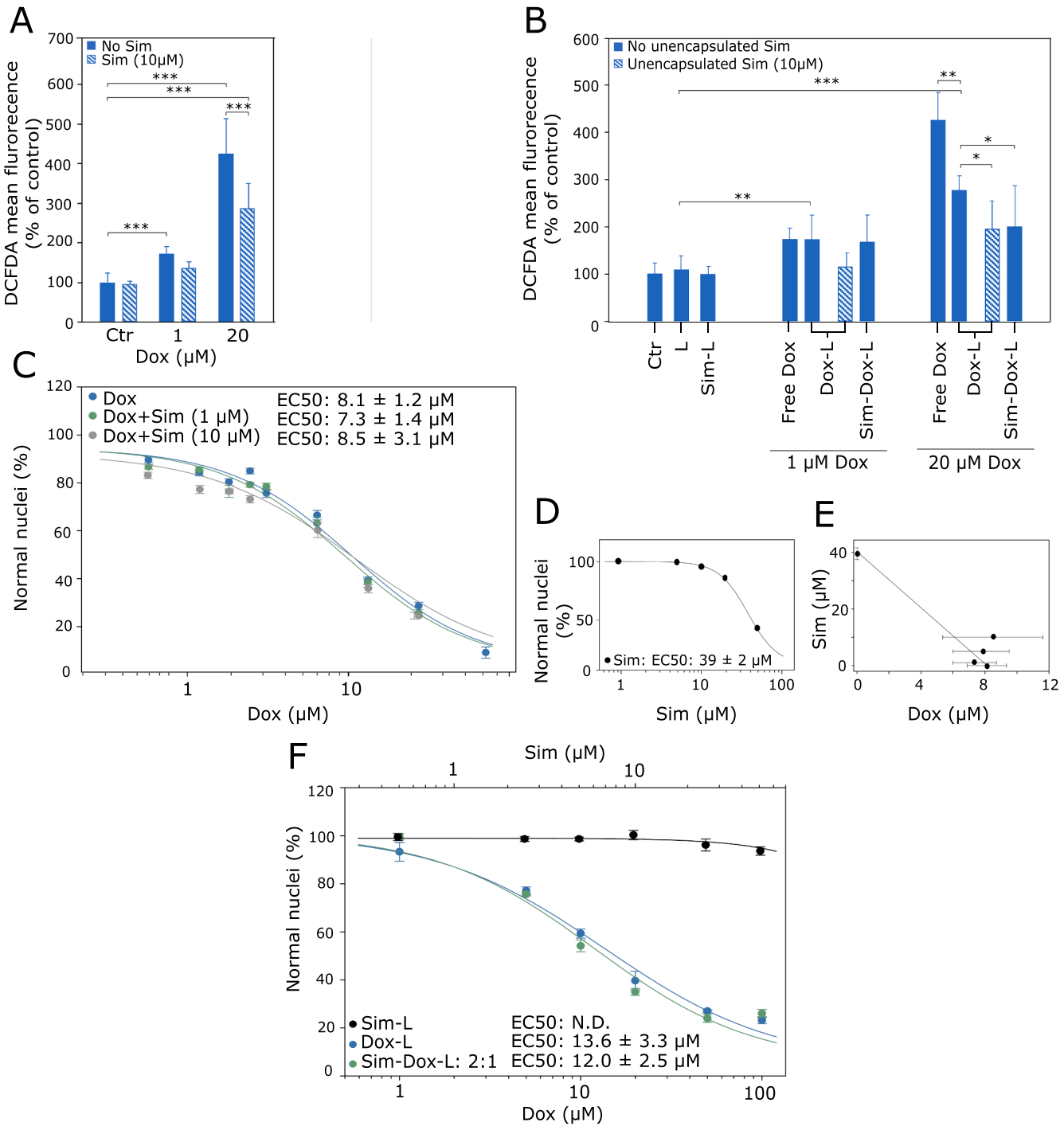

Fig. 2. The Cardioprotective Effect of Simvastatin in H9c2 Cardiomyoblasts. H9c2 cells were seeded at 5 × 10^4 cells/mL and left to attach for 24 h. A and B: Cells were incubated with 25 μM DCFDA for 30 min. before being pre-treated with Sim or corresponding control for 4 h prior to adding unencapsulated or liposomal Dox. Reactive oxygen species (ROS) levels were measured using a fluorescent plate reader four hours thereafter. C-D and E: H9c2 cells were treated with unencapsulated drugs (C and D) or liposomes (F) for 24 h. After treatment, microscopic evaluation of nuclear morphology was performed as described in the Methods section 2.4.3. EC_{50} values were determined by non-linear regression as described in the Methods section 2.6. E: Isobolographic plot obtained from the EC_{50} values for unencapsulated Sim and Dox to identify interactions. All data are presented as average of 6–9 experiments ± standard deviation. Statistics: One-way ANOVA with either LSD (equal variance) or Dunnett's T3 test (unequal variance). Variance was evaluated using Levene's test of homogeneity. L: empty liposomes, Sim-L: liposomal Sim, Dox-L: liposomal doxorubicin, Sim-Dox-L: liposomal Dox and Sim co-encapsulated, N.D: Not determined due to low cytotoxicity in the highest concentration tested.

Dox, 11.8 ± 1.5 μM, Fig. 6D) at non-toxic Sim concentrations. The CDI showed a potentiating effect of the co-encapsulation of the drugs.

4. Discussion

The cytotoxicity evoked by anti-cancer drugs such as anthracyclines are not limited to tumour cells but also affects normal cells and tissues, and can be the dose-limiting factor in cancer treatment (Swain et al.,

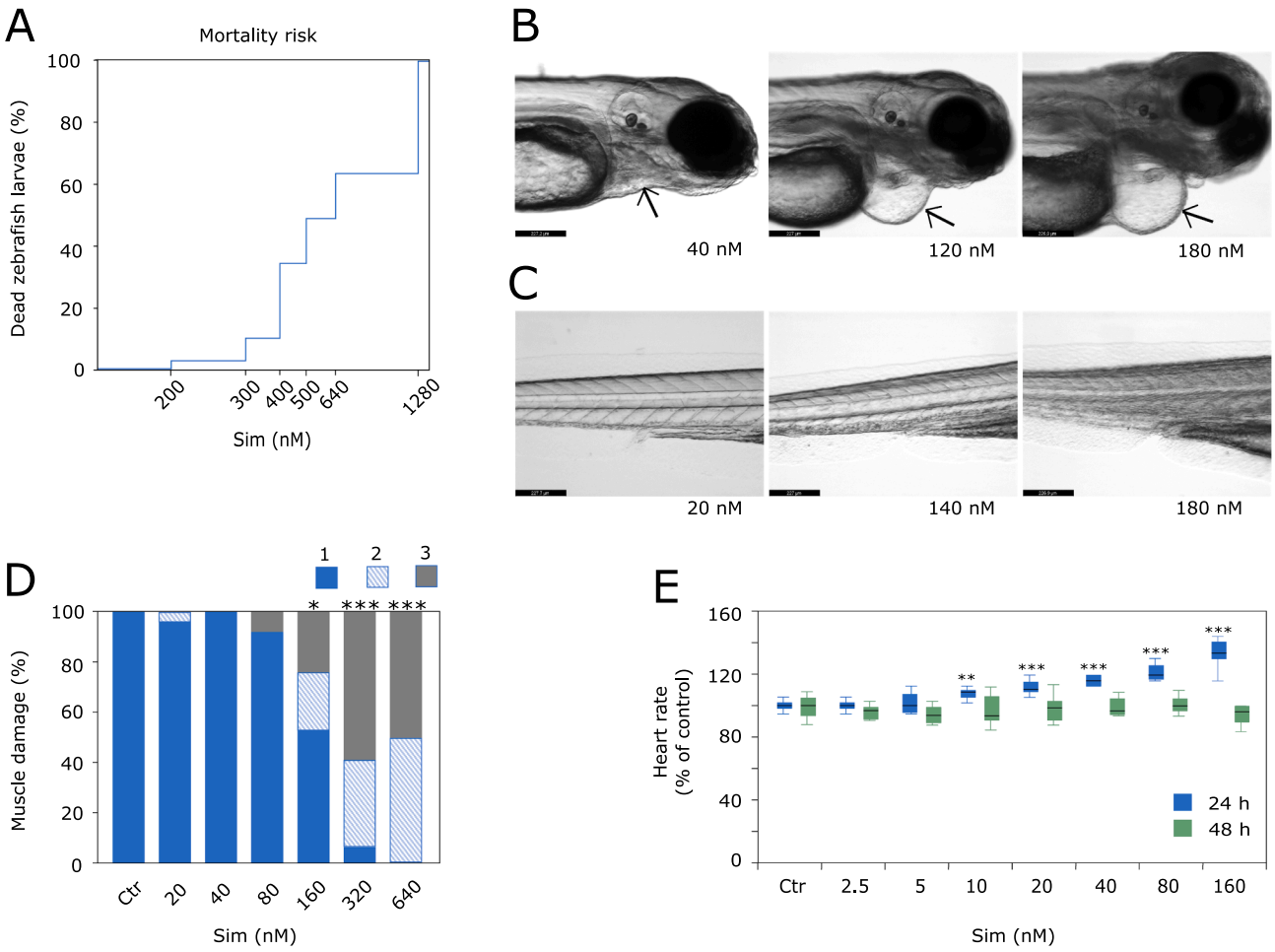

Fig. 3. The Toxic Effects of Sim on Zebrafish Larvae. Zebrafish larvae at the pec fin stage were exposed to simvastatin (Sim) in increasing concentrations dissolved in embryo water for 48 h. A: Mortality risk after 48 h Sim exposure (n = 5–15). B: Pericardial oedema after Sim exposure. The left image shows a larva with no oedema, while the middle and right images show increasing severity of pericardial oedema after Sim exposure. The arrows indicate the pericardial sac. C: Damage in tail skeletal muscle. Left to right: Grade 1: normal, 2: moderate and 3: severe. (Scale bars: 227 μm). D: Grade of skeletal muscle damage after 48 h of Sim exposure (n = 10–23). E: Heart rate after 24 and 48 h of continuous Sim exposure (n = 8–19). Statistics: One-way ANOVA with either LSD (equal variance) or Dunnett's T3 test (unequal variance) for the HR tests (E). Variance was evaluated using Levene's test of homogeneity. Kruskal-Wallis test was used for muscle damage score (D). Significance: $p \leq 0.05$ indicated by *, $p \leq 0.01$, by ** and $p \leq 0.001$, by ***.

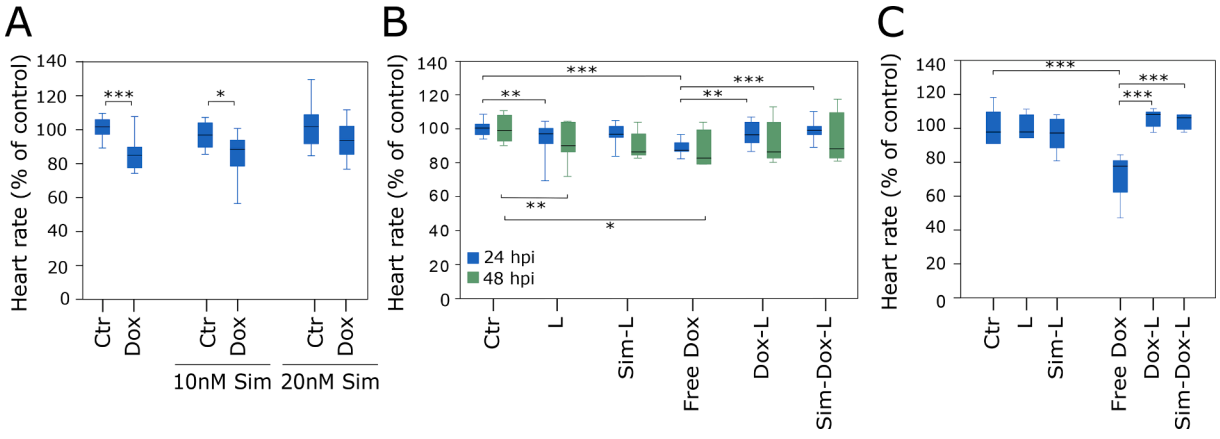

Fig. 4. The Cardioprotective Effect of Sim in Zebrafish Larvae exposed to Dox. A: Effects of unencapsulated simvastatin (Sim) and doxorubicin (Dox) on zebrafish larvae. Zebrafish larvae at the pec fin stage were exposed to 10 or 20 nM Sim in embryo water for 18 h before i.v. injection with either PBS (Ctr) or 2 ng Dox, and HR was assessed 24 h thereafter (n = 13–27). B and C: Effects of Intravenous injection of liposomal Dox and Sim on HR in zebrafish larvae. Zebrafish larvae were i.v. injected with PBS (Ctr), empty liposomes (L), Sim liposomes (Sim-L), free Dox, Dox liposomes (Dox-L) and Sim-Dox liposomes (Sim-Dox-L) at 55–65 hpf (B, n = 9–15) or at 55–65 hpf and 79–89 hpf (C, n = 4–6). Statistics: One-way ANOVA with either LSD (equal variance) or Dunnett's T3 test (unequal variance). Variance was evaluated using Levene's test of homogeneity. *$p < 0.05$, **$p < 0.01$, ***$p < 0.001$, non-significance is not marked.

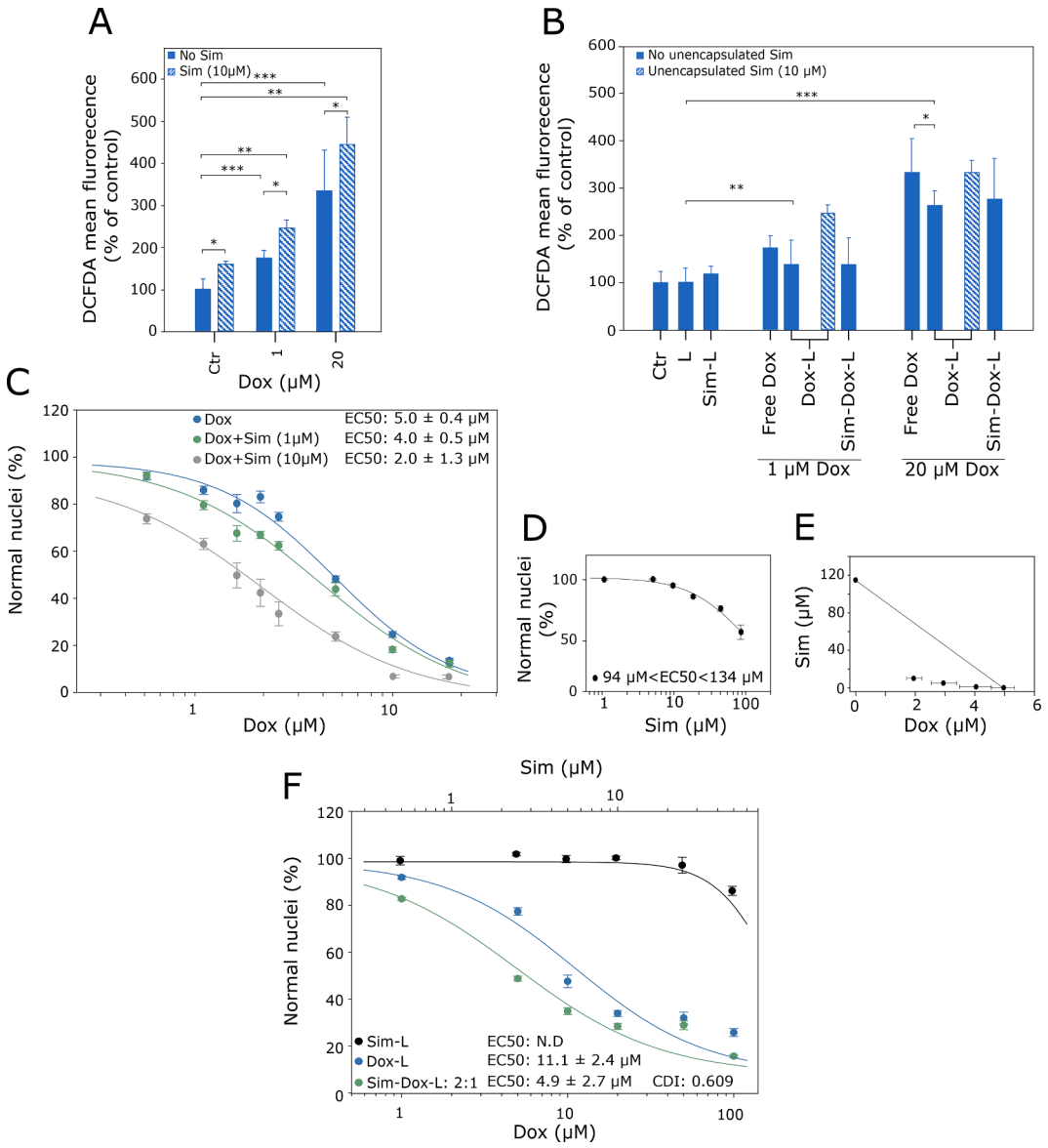

Fig. 5. Effect of Dox and Sim on ROS Generation and Cytotoxicity in the MCF7 Mammary Cancer Cell Line. MCF7 cells were seeded at 5×10^4 cells/mL and left to attach for 24 h. A and B: Cells were incubated with 25 μM DCFDA for 30 min. before the addition of drugs. Unencapsulated simvastatin (Sim) or corresponding control was added 4 h prior to the addition of doxorubicin (Dox) or liposomes. ROS levels was measured using a fluorescent plate reader 6 h (A) and 4 h (B) thereafter. C, D and F: MCF7 cells were treated with drugs or liposomes for 24 h before microscopic evaluation of nuclear morphology as described in the Methods section 2.4.3. EC_{50} values were determined by non-linear regression as described in the Methods section 2.6, except in D, where it was estimated based on the cytotoxic effect of the highest concentration. E: Isobolographic plot obtained from the EC_{50} values for both drugs to identify interactions. All data are presented as average ± standard deviation (C-E: n = 9, F: n = 6). Significance was calculated using one-way ANOVA with Dunnett's T3 post-hoc test and students *t*-test for CDI. *p < 0.05, **p < 0.01, ***p < 0.001. L: empty liposomes, Sim-L: liposomal Sim, Dox-L: liposomal doxorubicin, Sim-Dox-L: liposomal Dox and Sim co-encapsulated, N.D: Not determined due to low cytotoxicity in the highest concentration tested.

2003). In this study, we investigated the cardioprotective and anti-cancer effects of Sim in Dox therapy and developed PEGylated liposomes co-loaded with Sim and Dox to further attenuate the cardiotoxic effects of Dox while retaining the anti-cancer potency.

Sim and Dox was encapsulated into the liposomes at two different steps of the production, which allowed for manipulation of the loading ratio of the two drugs. We needed to be able to adjust the loading of Sim in the liposomes, since liposomal Sim appeared to be more toxic to zebrafish larvae than to the H9c2 cells (Figs. 2 and 3), presumably due to the higher demand of steroid synthesis during early zebrafish development (Campos et al., 2016). In line with other findings (Niu et al., 2010; Myhren et al., 2014), we achieved an encapsulation of more than 90 % of the added Dox inside the liposomes (Fig. S1). We noted that the drug loading of Sim decreased after Dox loading for the liposomes with the highest concentration of Sim (Table 2). This could be caused by Sim leaking out when the liposomes were reheated to above the transition temperature of HEPC when loading Dox.

Determination of liposome size by TEM resulted in lower diameters compared to DLS (Fig. 1). This could be caused by aggregation of liposomes in the suspension resulting in the DLS registering a larger particle size. Such aggregations may not be possible to observe in the TEM samples. Furthermore, it could be that the larger liposomes did not adhere as well to the formvar membrane on TEM grid, and that smaller liposomes may be overrepresented in the images in Fig. 1C and D. However, it is documented that DLS tend to over-estimate the relative number of larger particles in a population (for a recent review discussing this, see Farkas and Kramar, 2021), which will cause a shift towards larger liposome size compared to what is seen by TEM measurements.

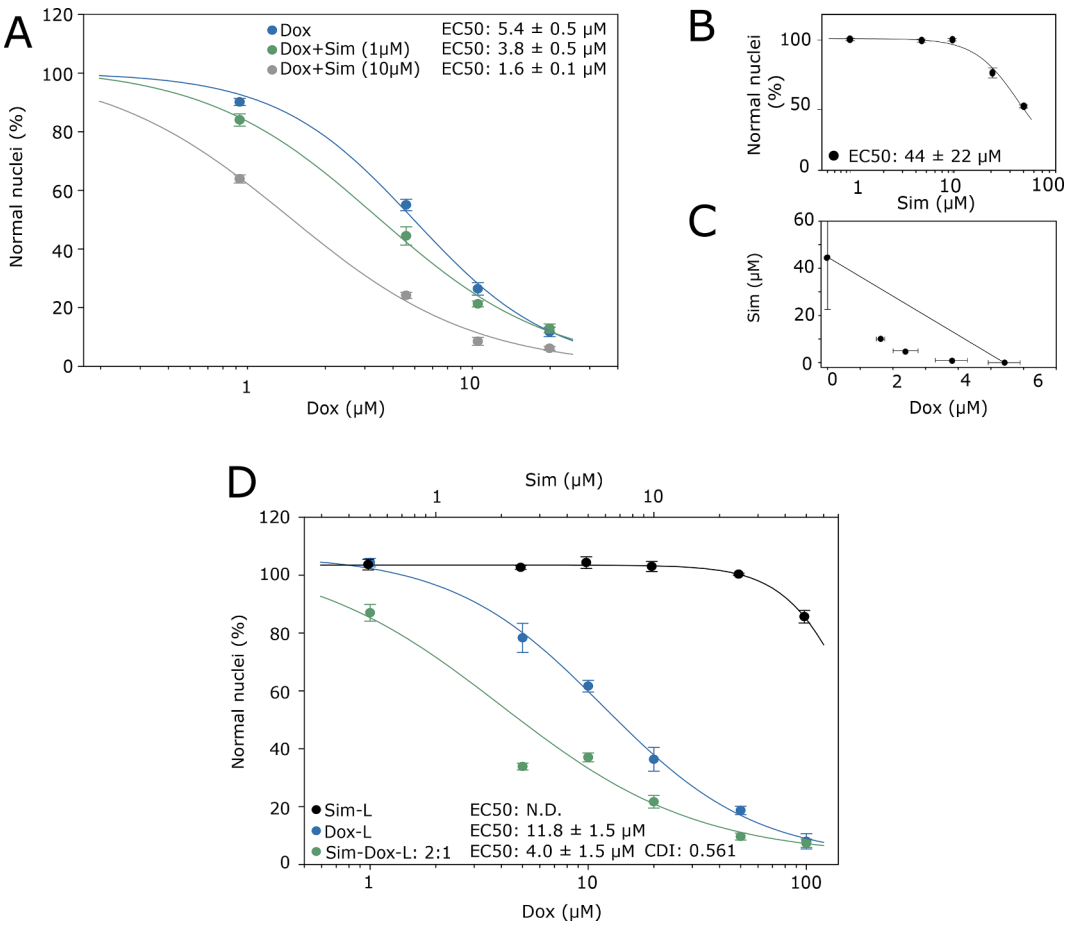

Fig. 6. The Cytotoxicity of Sim and Dox on the PC3 Prostate Adenocarcinoma Cell Line. A, B and D: PC3 cells were seeded at 5×10^4 cells/mL and left to attach for 24 h. The cells were treated with drugs or liposomes for 24 h before microscopic evaluation of nuclear morphology was performed as described in the Methods section 2.4.3. EC_{50} values were determined by non-linear regression as described in the Methods section 2.6. C: Drug combination analysis obtained from the EC_{50} values for both drugs to identify interactions. All data are presented as average ± standard deviation (A-C: n = 9, D: n = 6). Sim-L: liposomal Sim, Dox-L: liposomal doxorubicin, Sim-Dox-L: liposomal Dox and Sim co-encapsulated, N.D: Not determined due to low cytotoxicity in the highest concentration tested.

The ideal size range of liposomes to achieve tumour accumulation and prolonged circulation time is reported to be between 90 and 200 nm (Nagayasu et al., 1999). Our liposomes were within this range both when analysing via TEM and DLS, with a size of 100–115 nm and 140–180 nm, respectively and the size was not compromised by the incorporation of Dox (Table 2 and Fig. 1). The polydispersity index was at or lower than 0.10 for all liposomes (Table 2), which is regarded acceptable in pharmaceutical formulations (Danaei et al., 2018). Additionally, we added PEG-conjugated lipids to our liposomal formulations, to prolong circulation time of the liposomes. Similar sized PEGylated liposomes have been demonstrated to circulate in zebrafish larvae for up to 72 hpi, while un-PEGylated were not visible in the circulation 24 hpi (Evensen et al., 2016).

We found that Sim reduced Dox-induced ROS generation in H9c2 cardiomyoblasts but not cytotoxicity (Fig. 2A and C). This suggests that the cytotoxicity seen in vitro may not be the directly linked to elevated ROS, at least at the incubation times used in our experiment. Importantly though, Sim protected against Dox-induced reduced HR in zebrafish larvae (Fig. 4A). Apparently, the cytotoxicity seen in an in vitro model like H9c2-cells (Fig. 2) do not reflect the cardiotoxic events seen in patients. Cardiotoxicity is caused by several mechanisms that work in concert (Octavia et al., 2012). As such, we conclude that the zebrafish larva represents a better suited model system for Dox-induced cardiotoxicity compared to cardiomyoblast cytotoxicity.

An important aspect of potential cardioprotectants in Dox-treatment is that they do not impair the anti-cancer properties of the therapy. It has been reported that the cardioprotective agent dexrazoxane reduces the therapeutic efficacy of anthracyclines (European Medicines Agency, 2011). In contrast to this, we found that Sim increased ROS in MCF7 mammary cancer cells (Fig. 5A) and potentiated the cytotoxic effect of Dox in MCF7 cells as well as the PC3 prostate cancer cells (Fig. 5C-G and 6). Importantly this was achieved with concentrations of Sim which were not cytotoxic towards cardiomyoblasts or cancer cells (Figs. 2, 5 and 6). Previous reports on synergistic effects of Sim and Dox have used concentrations up to 50 μM of Sim which were toxic to cancer cells (Buranrat et al., 2017), but these concentrations were toxic to H9c2 cells in our tests (Fig. 2C), and likely to damage also the intact heart. Importantly, high concentrations also caused toxic responses in zebrafish larvae, evidenced by muscle damage, pericardial oedema, and increased lethality (Fig. 3). Statin associated myopathy in humans correlates with serum concentration (Thompson et al., 2006), and it is therefore important to maintain a low concentration in the blood to avoid this. By nanoencapsulation into liposomes, the level of free SIM will be kept at a minimum, and this could protect from harmful effects of the drug.

For our Dox and Sim co-loaded liposomes to be beneficial in cancer therapy, they need to retain the same cardioprotective properties as the free drug combination, while still being active towards the cancer cells. Both the Dox and Sim-Dox liposomal formulations reduced cardiomyoblast toxicity compared to free Dox (Fig. 2). Moreover, while encapsulation of PLD significantly reduced ROS generation in H9c2 cardiomyoblasts compared to unencapsulated Dox, this was further

reduced for H9c2 treated with our Sim-Dox liposomes (Fig. 2B). This demonstrates our previous notion that liposomes co-loaded with Sim and Dox can reduce Dox-induced cardiotoxicity beyond what is possible by encapsulation of Dox alone. Zebrafish larvae treated with PLD had the same heart rate as those treated with empty liposomes (Fig. 4B and C), suggesting that Dox is well retained inside the liposomes after injection, and do not leak out to cause cardiotoxic effects. Thus, in our systems, liposomal encapsulation was sufficient to protect against Dox-induced reduced HR. Importantly, co-encapsulation of Dox and Sim in the same liposomes led to significantly reduced viability for MCF7 and PC3 cells compared to liposomes loaded with Dox alone (Fig. 5F and 6D). This means that the Dox-potentiating effect observed for unencapsulated Sim is conserved in the Sim-Dox liposomes.

Taken together, our liposomal formulation could provide several advantages in delivery of Sim and Dox for combination therapy. First, it protects normal tissues from harmful effects of the two drugs. Secondly, it ensures co-delivery of the two drugs, which is important, both for cardioprotection, and for the anti-cancer effect. Lastly, liposomal formulation protects Sim from rapid elimination by liver metabolism and provides stable plasma-concentrations of the drug to exert both cardioprotective and anti-cancer effects.

Judging from the increased popularity of combination therapies in cancer, it is likely that the next generation of liposomes carries two or more drugs acting synergistically in cancer treatment. A recent example is Vyxeos® which gained FDA approval in 2017 for treatment of acute myeloid leukaemias associated with poor prognosis (Krauss et al., 2019). Vyexos® is a liposomal formulation containing both daunorubicin and cytarabine which have been used in combination against acute myeloid leukaemia for decades (Yates et al., 1973). The liposomal formulation increased survival in the tested patient groups compared to treatment with the two drugs separately (Krauss et al., 2019). It has been argued that despite the reduced toxicities associated with the use of PLD, clinical trials have not identified an enhanced anti-cancer activity compared to free Dox, and for PLD to be appreciated it must show an improved therapeutic index (Waterhouse et al., 2001). This can hopefully be achieved by co-encapsulating a drug like Sim together with Dox in the liposomes. The protective effect of Sim in Dox-induced cardiotoxicity (clinicaltrials.gov, NCT02096588) and the potentiating effect suggested here and by others (Feleszko et al., 2000; Buranrat et al., 2017; Werner et al., 2013; Feleszko et al., 1998), is likely to be improved by co-encapsulation of the drugs into liposomes, which will allow for synchronizing and controlling the biodistribution and delivery of the drugs to the tissues (Zucker and Barenholz, 2010), leading to a dual effect in cancer treatment with enhanced cardioprotection and anti-cancer effect.

CRediT authorship contribution statement

Ronja Bjørnstad: Conceptualization, Methodology, Formal analysis, Investigation, Writing – original draft, Visualization. **Ingeborg Nerbø Reiten:** Conceptualization, Methodology, Formal analysis, Investigation, Writing – original draft, Writing – review & editing, Visualization. **Kaja Skålnes Knudsen:** Investigation, Visualization. **Jan Schjøtt:** Conceptualization, Supervision, Writing – review & editing. **Lars Herfindal:** Conceptualization, Methodology, Validation, Formal analysis, Resources, Supervision, Project administration, Funding acquisition.

Declaration of Competing Interest

The authors declare that they have no known competing financial interests or personal relationships that could have appeared to influence the work reported in this paper.

Data availability

Data will be made available on request.

Acknowledgements

The authors would like to thank the Zebrafish Facility at the Department of Biological Sciences, University of Bergen for access to zebrafish embryos and embryo water. This project was financially supported by the Norwegian Western Region Health Authorities to Lars Herfindal (Grant No. 912052), Ronja Bjørnstad (Grant No. 912028), the Norwegian Society for Children's Cancer to Lars Herfindal (Grant Nos. 180007 and 190004), the University of Bergen with grant to Ingeborg Nerbø Reiten (Grant No. 100234103) and Astri og Edvard Riisøens legat to Lars Herfindal.

Appendix A. Supplementary material

Supplementary data to this article can be found online at https://doi.org/10.1016/j.ijpharm.2022.122379.

References

Acar, Z., Kale, A., Turgut, M., Demircan, S., Durna, K., Demir, S., et al., 2011. Efficiency of atorvastatin in the protection of anthracycline-induced cardiomyopathy. J. Am. Coll. Cardiol. 58 (9), 988–989.

Alexander, J., Dainiak, N., Berger, H.J., Goldman, L., Johnstone, D., Reduto, L., et al., 1979. Serial assessment of doxorubicin cardiotoxicity with quantitative radionuclide angiocardiography. N. Engl. J. Med. 300 (6), 278–283.

Alonso, D.F., Farina, H.G., Skilton, G., Gabri, M.R., De Lorenzo, M.S., Gomez, D.E., 1998. Reduction of mouse mammary tumor formation and metastasis by lovastatin, an inhibitor of the mevalonate pathway of cholesterol synthesis. Breast Can. Res. Treat. 50 (1), 83–93.

Angsutararux, P., Luanpitpong, S., Issaragrisil, S., 2015. Chemotherapy-induced cardiotoxicity: overview of the roles of oxidative stress. Oxid. Med. Cell Longev. 2015, 795602.

Bambino, K., Chu, J., 2017. Zebrafish in Toxicology and Environmental Health. Curr. Top. Dev. Biol. 124, 331–367.

Bansal, N., Adams, M.J., Ganatra, S., Colan, S.D., Aggarwal, S., Steiner, R., et al., 2019. Strategies to prevent anthracycline-induced cardiotoxicity in cancer survivors. Cardio-Oncology. 5 (1), 18.

Bansal, N., Adams, M.J., Ganatra, S., Colan, S.D., Aggarwal, S., Steiner, R., et al., 2019. Strategies to prevent anthracycline-induced cardiotoxicity in cancer survivors. Cardiooncology. 5, 18.

Barenholz, Y., 2012. Doxil®–the first FDA-approved nano-drug: lessons learned. J. Control. Release 160 (2), 117–134.

Bjørnstad, R., Aesoy, R., Bruserud, Ø., Brenner, A.K., Giraud, F., Dowling, T.H., et al., 2019. A kinase inhibitor with anti-Pim kinase activity is a potent and selective cytotoxic agent toward acute myeloid leukemia. Mol. Cancer Ther. 18 (3), 567–578.

Blais, L., Desgagné, A., LeLorier, J., 2000. 3-Hydroxy-3-methylglutaryl coenzyme A reductase inhibitors and the risk of cancer: a nested case-control study. Arch. Intern. Med. 160 (15), 2363–2368.

Buranrat, B., Suwannaloet, W., Naowaboot, J., 2017. Simvastatin potentiates doxorubicin activity against MCF-7 breast cancer cells. Oncol Lett. 14 (5), 6243–6250.

Campos, L.M., Rios, E.A., Guapyassu, L., Midlej, V., Atella, G.C., Herculano-Houzel, S., et al., 2016. Alterations in zebrafish development induced by simvastatin: comprehensive morphological and physiological study, focusing on muscle. Exp. Biol. Med. (Maywood). 241 (17), 1950–1960.

Cappetta, D., De Angelis, A., Sapio, L., Prezioso, L., Illiano, M., Quaini, F., et al., 2017. Oxidative stress and cellular response to doxorubicin: a common factor in the complex milieu of anthracycline cardiotoxicity. Oxid. Med. Cell Longev. 2017, 1521020.

Crick, D.C., Andres, D.A., Danesi, R., Macchia, M., Waechter, C.J., 1998. Geranylgeraniol overcomes the block of cell proliferation by lovastatin in C6 glioma cells. J. Neurochem. 70 (6), 2397–2405.

D'Agati, G., Beltre, R., Sessa, A., Burger, A., Zhou, Y., Mosimann, C., et al., 2017. A defect in the mitochondrial protein Mpv17 underlies the transparent casper zebrafish. Dev. Biol. 430 (1), 11–17.

Danaei, M., Dehghankhold, M., Ataei, S., Hasanzadeh Davarani, F., Javanmard, R., Dokhani, A., et al., 2018. Impact of particle size and polydispersity index on the clinical applications of lipidic nanocarrier systems. Pharmaceutics. 10 (2).

Davies, K.J., Doroshow, J.H., 1986. Redox cycling of anthracyclines by cardiac mitochondria. I. Anthracycline radical formation by NADH dehydrogenase. J. Biol. Chem. 261 (7), 3060–3067.

Dyballa, S., Miñana, R., Rubio-Brotons, M., Cornet, C., Pederzani, T., Escaramis, G., et al., 2019. Comparison of zebrafish larvae and hiPSC cardiomyocytes for predicting drug induced cardiotoxicity in humans. Toxicol. Sci. 171 (2), 283–295.

European Medicines Agency, 2011. Assessment report Dexrazoxane-containing medicinal products (EMA/775079/2011) London, UK: European Medicines Agency; [cited 2021 May 20.].

Evensen, L., Johansen, P.L., Koster, G., Zhu, K., Herfindal, L., Speth, M., et al., 2016. Zebrafish as a model system for characterization of nanoparticles against cancer. Nanoscale. 8 (2), 862–877.

Farina, H.G., Bublik, D.R., Alonso, D.F., Gomez, D.E., 2002. Lovastatin alters cytoskeleton organization and inhibits experimental metastasis of mammary carcinoma cells. Clin. Exp. Metastasis 19 (6), 551–559.
Farkas, N., Kramar, J.A., 2021. Dynamic light scattering distributions by any means. J. Nanopart. Res. 23 (5), 120.
Feleszko, W., Zagozdzon, R., Gołab, J., Jakóbisiak, M., 1998. Potentiated antitumour effects of cisplatin and lovastatin against MmB16 melanoma in mice. Eur. J. Cancer 34 (3), 406–411.
Feleszko, W., Mlynarczuk, I., Balkowiec-Iskra, E.Z., Czajka, A., Switaj, T., Stoklosa, T., et al., 2000. Lovastatin potentiates antitumor activity and attenuates cardiotoxicity of doxorubicin in three tumor models in mice. Clin. Cancer Res. 6 (5), 2044–2052.
Fritze, A., Hens, F., Kimpfler, A., Schubert, R., Peschka-Süss, R., 2006. Remote loading of doxorubicin into liposomes driven by a transmembrane phosphate gradient. Biochim. Biophys. Acta, Rev. Cancer 1758 (10), 1633–1640.
Ganatra, S., Nohria, A., Shah, S., Groarke, J.D., Sharma, A., Venesy, D., et al., 2019. Upfront dexrazoxane for the reduction of anthracycline-induced cardiotoxicity in adults with preexisting cardiomyopathy and cancer: a consecutive case series. Cardio-Oncol. 5 (1), 1.
Gessner, P.K., 1988. A straightforward method for the study of drug interactions: an isobolographic analysis primer. J. Am. College Toxicol. 7 (7), 26.
Gewirtz, D.A., 1999. A critical evaluation of the mechanisms of action proposed for the antitumor effects of the anthracycline antibiotics adriamycin and daunorubicin. Biochem. Pharmacol. 57 (7), 727–741.
Goffart, S., von Kleist-Retzow, J.-C., Wiesner, R.J., 2004. Regulation of mitochondrial proliferation in the heart: power-plant failure contributes to cardiac failure in hypertrophy. Cardiovasc. Res. 64 (2), 198–207.
Graaf, M.R., Beiderbeck, A.B., Egberts, A.C., Richel, D.J., Guchelaar, H.J., 2004. The risk of cancer in users of statins. J. Clin. Oncol. 22 (12), 2388–2394.
Henninger, C., Fritz, G., 2017. Statins in anthracycline-induced cardiotoxicity: Rac and Rho, and the heartbreakers. Cell Death Dis. 8 (1), e2564.
Islam, M.M., Yang, H.C., Nguyen, P.A., Poly, T.N., Huang, C.W., Kekade, S., et al., 2017. Exploring association between statin use and breast cancer risk: an updated meta-analysis. Arch. Gynecol. Obstet. 296 (6), 1043–1053.
Jakóbisiak, M., Bruno, S., Skierski, J.S., Darzynkiewicz, Z., 1991. Cell cycle-specific effects of lovastatin. Proc. Natl. Acad. Sci. USA 88 (9), 3628–3632.
Kimmel, C.B., Ballard, W.W., Kimmel, S.R., Ullmann, B., Schilling, T.F., 1995. Stages of embryonic development of the zebrafish. Dev. Dyn. 203 (3), 253–310.
Krauss, A.C., Gao, X., Li, L., Manning, M.L., Patel, P., Fu, W., et al., 2019. FDA approval summary: (daunorubicin and cytarabine) liposome for injection for the treatment of adults with high-risk acute myeloid leukemia. Clin. Cancer Res. 25 (9), 2685–2690.
Lefrak, E.A., Piťha, J., Rosenheim, S., Gottlieb, J.A., 1973. A clinicopathologic analysis of adriamycin cardiotoxicity. Cancer 32 (2), 302–314.
Liao, J.K., Laufs, U., 2005. Pleiotropic effects of statins. Annu. Rev. Pharmacol. Toxicol. 45, 89–118.
Maciag, M., Wnorowski, A., Mierzejewska, M., Plazinska, A., 2022. Pharmacological assessment of zebrafish-based cardiotoxicity models. Biomed. Pharmacother. 148, 112695.
Maltese, W.A., Sheridan, K.M., 1985. Differentiation of neuroblastoma cells induced by an inhibitor of mevalonate synthesis: relation of neurite outgrowth and acetylcholinesterase activity to changes in cell proliferation and blocked isoprenoid synthesis. J. Cell. Physiol. 125 (3), 540–558.
Mueck, A.O., Seeger, H., Wallwiener, D., 2003. Effect of statins combined with estradiol on the proliferation of human receptor-positive and receptor-negative breast cancer cells. Menopause 10 (4), 332–336.
Myhren, L., Nilssen, I.M., Nicolas, V., Døskeland, S.O., Barratt, G., Herfindal, L., 2014. Efficacy of multi-functional liposomes containing daunorubicin and emetine for treatment of acute myeloid leukaemia. Eur. J. Pharm. Biopharm. 88 (1), 186–193.
Nagayasu, A., Uchiyama, K., Kiwada, H., 1999. The size of liposomes: a factor which affects their targeting efficiency to tumors and therapeutic activity of liposomal antitumor drugs. Adv. Drug Deliv. Rev. 40 (1–2), 75–87.
Niu, G., Cogburn, B., Hughes, J., 2010. Preparation and characterization of doxorubicin liposomes. Methods Mol. Biol. 624, 211–219.
O'Brien, M.E., Wigler, N., Inbar, M., Rosso, R., Grischke, E., Santoro, A., et al., 2004. Reduced cardiotoxicity and comparable efficacy in a phase III trial of pegylated liposomal doxorubicin HCl (CAELYX/Doxil) versus conventional doxorubicin for first-line treatment of metastatic breast cancer. Ann. Oncol. 15 (3), 440–449.
Octavia, Y., Tocchetti, C.G., Gabrielson, K.L., Janssens, S., Crijns, H.J., Moens, A.L., 2012. Doxorubicin-induced cardiomyopathy: from molecular mechanisms to therapeutic strategies. J. Mol. Cell. Cardiol. 52 (6), 1213–1225.
Park, C., Lee, I., Kang, W.K., 2001. Lovastatin-induced E2F–1 modulation and its effect on prostate cancer cell death. Carcinogenesis 22 (10), 1727–1731.
Rao, S., Porter, D.C., Chen, X., Herliczek, T., Lowe, M., Keyomarsi, K., 1999. Lovastatin-mediated G1 arrest is through inhibition of the proteasome, independent of hydroxymethyl glutaryl-CoA reductase. Proc. Natl. Acad. Sci. USA 96 (14), 7797–7802.
Riad, A., Bien, S., Westermann, D., Becher, P.M., Loya, K., Landmesser, U., et al., 2009. Pretreatment with statin attenuates the cardiotoxicity of doxorubicin in mice. Cancer Res. 69 (2), 695–699.
Saraste, A., Pulkki, K., 2000. Morphologic and biochemical hallmarks of apoptosis. Cardiovasc. Res. 45 (3), 528–537.
Schachter, M., 2005. Chemical, pharmacokinetic and pharmacodynamic properties of statins: an update. Fundam Clin Pharmacol 19 (1), 117–125.
Schneider, C.A., Rasband, W.S., Eliceiri, K.W., 2012. NIH Image to ImageJ: 25 years of image analysis. Nat. Methods 9 (7), 671–675.
Seeger, H., Wallwiener, D., Mueck, A.O., 2003. Statins can inhibit proliferation of human breast cancer cells in vitro. Exp. Clin. Endocrinol. Diabetes 111 (1), 47–48.
Shai, A., Rennert, H.S., Lavie, O., Ballan-Haj, M., Bitterman, A., Steiner, M., et al., 2014. Statins, aspirin and risk of venous thromboembolic events in breast cancer patients. J. Thromb. Thrombolysis 38 (1), 32–38.
Singh, S., Singh, P.P., Singh, A.G., Murad, M.H., Sanchez, W., 2013. Statins are associated with a reduced risk of hepatocellular cancer: a systematic review and meta-analysis. Gastroenterology 144 (2), 323–332.
Speyer, J.L., Green, M.D., Zeleniuch-Jacquotte, A., Wernz, J.C., Rey, M., Sanger, J., et al., 1992. ICRF-187 permits longer treatment with doxorubicin in women with breast cancer. J. Clin. Oncol. 10 (1), 117–127.
Swain, S.M., Whaley, F.S., Gerber, M.C., Weisberg, S., York, M., Spicer, D., et al., 1997. Cardioprotection with dexrazoxane for doxorubicin-containing therapy in advanced breast cancer. J. Clin. Oncol. 15 (4), 1318–1332.
Swain, S.M., Whaley, F.S., Ewer, M.S., 2003. Congestive heart failure in patients treated with doxorubicin: a retrospective analysis of three trials. Cancer 97 (11), 2869–2879.
Tan, P., Zhang, C., Wei, S.Y., Tang, Z., Gao, L., Yang, L., et al., 2017. Effect of statins type on incident prostate cancer risk: a meta-analysis and systematic review. Asian J. Androl. 19 (6), 666–671.
Tebbi, C.K., London, W.B., Friedman, D., Villaluna, D., Alarcon, P.A.D., Constine, L.S., et al., 2007. Dexrazoxane-associated risk for acute myeloid leukemia/myelodysplastic syndrome and other secondary malignancies in pediatric Hodgkin's disease. J. Clin. Oncol. 25 (5), 493–500.
Thompson, P.D., Clarkson, P.M., Rosenson, R.S., 2006. An assessment of statin safety by muscle experts. Am. J. Cardiol. 97 (8a), 69c–76c.
Wang, E.C., Wang, A.Z., 2014. Nanoparticles and their applications in cell and molecular biology. Integr. Biol. (Camb). 6 (1), 9–26.
Waterhouse, D.N., Tardi, P.G., Mayer, L.D., Bally, M.B., 2001. A comparison of liposomal formulations of doxorubicin with drug administered in free form: changing toxicity profiles. Drug Saf. 24 (12), 903–920.
Werner, M., Atil, B., Sieczkowski, E., Chiba, P., Hohenegger, M., 2013. Simvastatin-induced compartmentalisation of doxorubicin sharpens up nuclear topoisomerase II inhibition in human rhabdomyosarcoma cells. Naunyn Schmiedebergs Arch Pharmacol. 386 (7), 605–617.
Westerfield, M., 1995. The Zebrafish Book. A Guide for the Laboratory Use of Zebrafish (Danio rerio), 3rd edition. University of Oregon Press, Eugene, OR, pp. 385–pp.
Wolf, M.B., Baynes, J.W., 2006. The anti-cancer drug, doxorubicin, causes oxidant stress-induced endothelial dysfunction. Biochim. Biophys. Acta, Rev. Cancer 1760 (2), 267–271.
Wu, Q.J., Tu, C., Li, Y.Y., Zhu, J., Qian, K.Q., Li, W.J., et al., 2015. Statin use and breast cancer survival and risk: a systematic review and meta-analysis. Oncotarget. 6 (40), 42988–43004.
Yates, J.W., Wallace Jr., H.J., Ellison, R.R., Holland, J.F., 1973. Cytosine arabinoside (NSC-63878) and daunorubicin (NSC-83142) therapy in acute nonlymphocytic leukemia. Cancer Chemother Rep. 57 (4), 485–488.
Zhu, J.J., Xu, Y.Q., He, J.H., Yu, H.P., Huang, C.J., Gao, J.M., et al., 2014. Human cardiotoxic drugs delivered by soaking and microinjection induce cardiovascular toxicity in zebrafish. J. Appl. Toxicol. 34 (2), 139–148.
Zucker, D., Barenholz, Y., 2010. Optimization of vincristine-topotecan combination–paving the way for improved chemotherapy regimens by nanoliposomes. J. Control. Release 146 (3), 326–333.